5th International Conference on Industry 4.0 and Smart Manufacturing

Deep Fuzzy Cognitive Maps for Defect Inspection in Antenna Assembly

T. Tziolas[a], K. Papageorgiou[a], A. Feleki[a], T. Theodosiou[a], K. Rapti[a], E. Papageorgiou[a*]

S. Pantoja[b], A. Cuinas[b]

aUniversity of Thessaly, Dept. of Energy Systems, Gaiopolis, 41500 Larissa, Greece
bTeleves, Rúa B. de Conxo, 17 Santiago de Compostela, 15706, A Coruña, España

Abstract

Regardless of the tremendous technological development in manufacturing processes and equipment, assembly errors are an emerging concern. Hence, quality inspection software is of high importance for capturing defects at the source and preventing further error propagation. The advantages of Fuzzy Cognitive Maps (FCMs) as knowledge representation models with explainable capabilities can be compounded with the advantages of Deep Convolutional Neural Networks (CNNs) in order to acquire accurate and interpretable inspection results in Smart Manufacturing. In this work, an explainable binary classification approach is performed, namely DeepK-FCM, and appears to be able to assess sufficiently industrial images from TELEVES. The suggested DeepK-FCM methodology, inheriting the powerful characteristics of deep learning and FCMs, includes a number of steps as follows: fine-tuning of well-known CNNs for feature extraction with transfer learning, feature clustering by performing K-Means algorithm, definition of causal relationships through fuzzy measures on similarities produced and FCM model for the decision-making. Through the experimental analysis on a real industrial data set, it is being proved that the current approach with DeepK-FCM is more efficient for the task of defect inspection in the antenna assembly than the straightforward binary classification accomplished by CNNs. The attained accuracy of 80% is improved by 3% compared to the state-of-art CNN classifiers and indicates a high potential even when the data are scarce. In addition, the decision-making with FCMs levitates the interpretability of the system which contributes to the efforts towards a more explainable AI method for quality control inspection.

* Corresponding author. Tel.: +0-000-000-0000 ; fax: +0-000-000-0000 .
  E-mail address: elpinikipapageorgiou@uth.gr

1. Introduction

A frequent yet complex process in manufacturing is the assembly of disparate materials. Due to dissimilar resiliencies of the substances, assembly errors are rather frequent. Moreover, the upstream cause of deficiencies in a multi-stage production line is often opaque, and therefore the error is propagated and even amplified in each sequential processing step. This results in economic fallouts for the corporation. In smart manufacturing, machine vision systems have emerged to enhance the quality inspection procedure, which is evolving from an entirely manual practice to an Artificial Intelligence (AI)-driven task. These systems have been proven to be beneficial when compared to traditional manual performed inspections [1], as they can handle massive data and can be installed with ease in various stages of the production line; thus, capturing the error at its source.

Deep learning is a commonly employed AI method that has been successfully utilized in various manufacturing applications [2]. Convolutional Neural Networks (CNNs) are able to extract and select representative features from the input image, in an efficient and automatic way, thus alleviating the need for feature engineering, a commonly employed technique in several Machine Learning (ML) applications. On one hand, CNNs have achieved remarkable results in machine vision such as image classification. Researchers exploited ImageNet [3], a large computer vision database, to develop and propose efficient CNN models that can increase the performance metrics in this domain. Beyond the astonishing performance that has been achieved in ImageNet, these models continue to contribute to industrial applications and several other disciplines, as literature findings point out the generalization abilities of these models and the advantages of Transfer learning [4]. Among the proposed models, VGG16, VGG-19 [5] and ResNets [6] have been widely employed within the task of transfer learning. On the other hand, CNNs entail disadvantages that still need to be considered. A momentous concern regarding CNNs is their working principle which is considered a black box, as there is no indication of what is learned and how the decision is being made. Therefore, research efforts have been focused to tackle this limitation and to propose models with transparency in the decision-making [7], that will benefit industrial applications.

Fuzzy Cognitive Maps (FCMs) is a powerful transparent knowledge representation tool (graph-based) that was introduced by Kosko [8] and represents knowledge through states and processes. As the name suggests, an FCM consists of nodes/concepts and weighted arcs that describe the causality of a system using fuzziness. An important aspect of FCMs is the ability to incorporate both knowledge from experts and learning from data [9]. Hence, the advantageous characteristics of FCMs draw a lot of attention to the AI community, resulting in several works that have utilized them in a variety of industrial and engineering applications [9,10]. However, in pattern recognition and especially in image classification applying FCMs, there is still a research gap and opportunities for expansion towards explainable image processing. Moreover, FCMs' disadvantage in image processing is in line with other ML approaches, as they require feature engineering. To this end, efforts are focused on fusing the advantageous features of CNNs and FCMs for explainable and efficient image classification [11].

In this work, the compound of Deep CNNs, K-means and FCMs (DeepK-FCM) is performed for the task of image classification and quality inspection in a real industrial dataset. This work aims to distinguish antennas containing assembly defects from healthy ones, using a dataset derived from production monitoring in TELEVES. As data scarcity is inevitable in real industrial environments [12], data scarcity is closely linked to the employment of Data Augmentation (DA) and transfer learning techniques. The efficacy of DeepK-FCM is compared to the straightforward binary classification with CNNs and Transfer learning. The DeepK-FCM methodology not only manages to increase the accuracy of CNNs, but also mitigates the black box decision-making procedure as the obtained causal relationships among clusters and classes (called weight matrix) and the FCM inference process reveal the internal classification mechanism. Hence, the contribution of this work is a transparent classifier that increases the performance of traditional CNN approaches for the task of defect identification in a scarce industrial dataset.

2. Related Work

2.1. Deep Fuzzy Cognitive Maps for Image Classification

Significant scientific contributions have been made recently for the task of image classification with FCMs. In [11], a novel FCM scheme was proposed that utilizes the extracted features of a pre-trained VGG-16 network. The extracted features are then clustered with the fuzzy c-means algorithm to form semantic granules; in other words, a clustering algorithm is employed to group visual content that is being identified by VGG from the input image. The cluster centroids are the concepts of the FCM, and they represent the semantic concepts of the real world, as these are depicted in the corresponding images. The interconnections are then calculated using a similarity formula and fuzzy sets to estimate the similarity degree between each image feature and a cluster center. The method was tested in several open datasets and managed to increase the classification accuracy of CNNs with an interpretable result.

Another work that utilizes Deep CNNs and FCMs was found in [13]. In contrast to the previous one, the extracted features from the RetinaNet model are directly passed as concepts to the FCM. To establish the causal relationship between concepts, the Bird Swarm Intelligence Optimization algorithm was employed. Two benchmark datasets for the task of Remote Sensing Image classification were examined surpassing the results of different state-of-the-art approaches on these datasets.

In this research study, we built on top of the methodology that was presented in [11], due to its simplicity in implementation and low time consuming for classification tasks, by improving its interpretable capabilities in classification using FCM, following a way compatible to human logic. In addition, the semantic granules that employed in [11] present clearer concepts definition than the obscure extracted CNN features which are directly being passed as concepts in [13]. Furthermore, due to the peculiar properties of the industrial datasets in terms of defect class characteristics, CNN was fine-tuned in our work to ensure that meaningful features are extracted. To this end, an improved methodological approach based on [11] is implemented for an industrial case that further provides an interpretable FCM model with cause and effect relationships among concepts.

2.2. Theoretical Background of Fuzzy Cognitive Maps

FCMs are graph-based models for making decisions following a similar to the human decision-making process for the design and representation of complex systems. FCMs are an extension of cognitive maps and were proposed by Kosko in 1986 [8]. FCMs can extract knowledge from historical data and transform the extracted information into concepts/states and calculate the cause-and-effect relationships between them. The edges of the relationships/interconnections are directed and can be positive or negative, depending on the strength and the causality of the relationship. Regarding the edges between two concepts C_i and C_j, they take values from the fuzzy range [-1, 1], and if the value is $e_{i,j} = 0$, it is demonstrated that no causality exists between concepts, if $e_{i,j} < 0$ it is indicated that a negative causality exists, meaning if C_i decreases, then C_j increases. Lastly, if $e_{i,j} > 0$, it exhibits positive causality, more specifically if C_i increases, C_j increases as well [14–16]. FCMs consist of a weight matrix definition, which takes values in range [-1, 1]. Weight matrix relationships indicate the strength of the relationships between concepts [17].

Following the establishment of concepts and their interconnections, the calculation of future states is applied. For the FCM to converge, Equation (1) is utilized. At each iteration k, the value of the concept is influenced by the values of the connected concepts, and is updated according to Equation (1). Equation (1) utilizes Sigmoid as a transfer function f for the normalization of future states in the range [0, 1].

$$A_i^{(K+1)} = f\left(A_i^{(K)} + \sum_{i,j}^{N} w_{ij} A_j^{(K)}\right) \tag{1}$$

where, $A_i^{(K+1)}$ is the value of the concept iteration (k+1) and $A_j^{(K)}$ is the concept at the iteration (k) and f is the sigmoid function. The demand for transparent and explainable methods has escalated since the predicted outcomes from algorithms must be trustworthy. This drives the researchers to adjust explainability to Artificial Intelligence (AI) since AI's decisions have been applied in many domains.

3. Methodology

3.1. Dataset

A FLIR Blackfly S BFS-PGE-200S6C machine vision camera was installed directly in the antenna manufacturing line of Televes to monitor the assembly process. The sensor outputs RGB images of size 4401×2898 pixels. A dataset was gathered and annotated into two classes {defective, healthy}, or equivalently {0,1}, by the experts on the shopfloor. Each image in the dataset corresponds to a unique part. The total parts that were examined are 327 healthy and 120 defective. Subsequently, the splitting into training-testing sub-datasets was performed. A balanced sub-dataset of 36 images per class (72 total images) is kept for testing to ensure that the model generalizes well in both classes and does not overfit in the majority class. The training sub-dataset consists of 291 healthy and 84 defective parts, which indicates a 3.4 to 1 imbalance ratio for the healthy class. The data imbalance is counteracted with different class weights during training; Hence, higher weight is passed to the minority class to further penalize its misclassifications. An indicative example of healthy/defective parts is presented in Fig. 1. It is observed that the defect class contains housing deformations from the poor insertion of the metallic rod, as well as cracked parts from material failure.
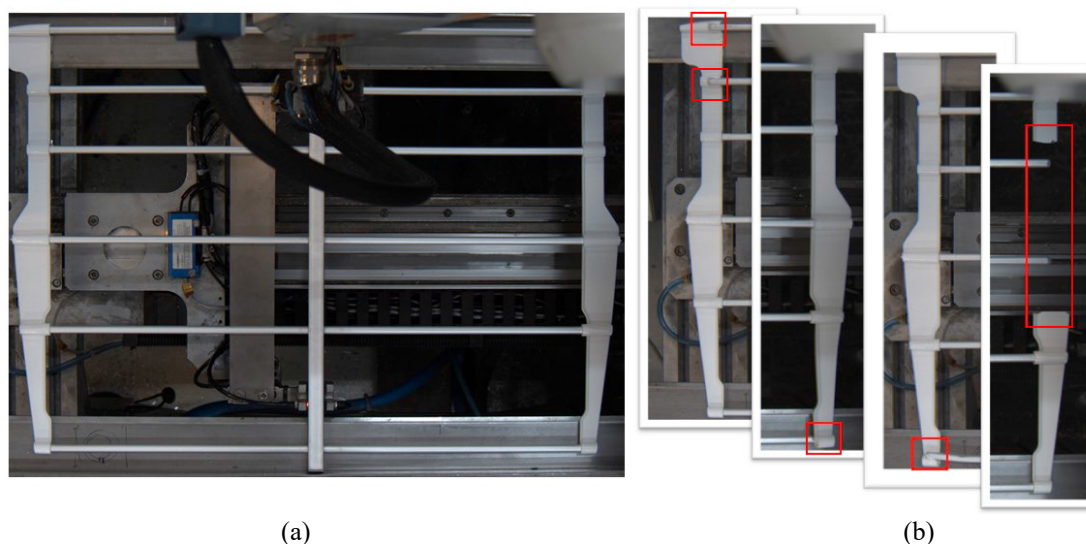

(a)   (b)

Fig. 1. Indicative parts: (a) Healthy; (b) Defective.

3.2. DeepK-FCM framework

The DeepK-FCM model employs an innovative approach for image classification in a real industrial domain, incorporating FCM models with explainable capabilities. In the proposed DeepK-FCM framework, the FCM methodology is attained along with Fuzzy Logic and semantic granules, in order to construct an interpretable graph-based model. The main aspects of feature extraction from CNNs and construction of semantic granules after feature clustering are employed. The image data have been processed by the trained ResNet-101 model (as the most efficient state of the art CNN model). The proposed model does not depend on experts' knowledge. On the contrary, it employs exclusively the knowledge from the dataset of images, where it clusters the features that belong to the same class, extracted from CNN [18]. More specifically, the model utilizes the knowledge extracted from the calculated similarities between image representations and the centroids from the generated clusters. The input concepts of the proposed model are demonstrated from the calculated centroids and the output concepts are the output classes. DeepK-FCM consists of four processing steps for explainable decision making that are further described in the following subsections. Moreover, the overall workflow of the DeepK-FCM is presented in Fig. 2. An example of the produced FCM model for the corresponding image dataset is included this figure.
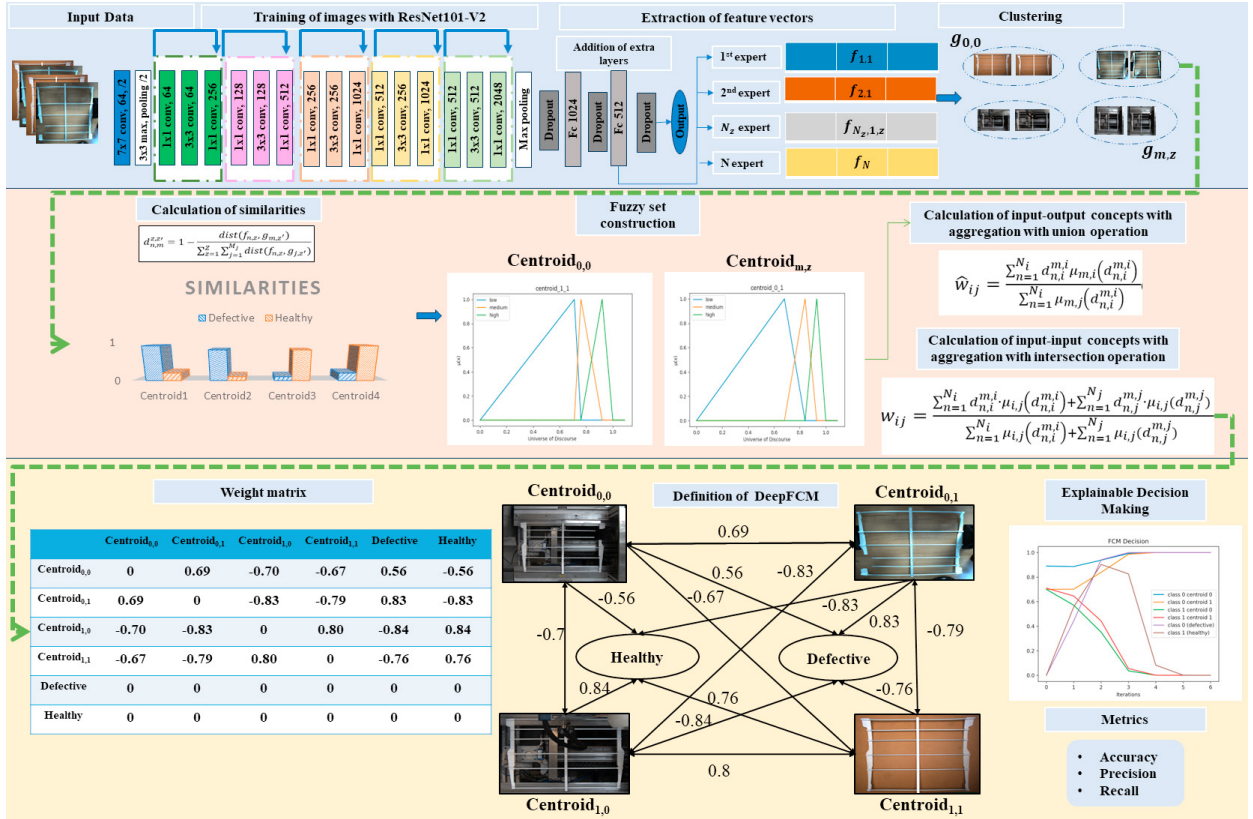
Fig. 2. The proposed DeepK-FCM methodology for image classification.

Step 1.   Data preprocessing

Initially, the data are preprocessed. This includes resizing images to a smaller size that will reduce the computations without sacrificing the accuracy of the model. The size of 600×600 pixels and the bilinear resizing method were experimentally chosen following a trial and error approach with selection of the appropriate parameters. Consequently, Data Augmentation (DA) techniques were employed in the training dataset to alleviate data scarcity. The DA techniques utilized in this work include random geometric transformations (rotations and flipping) and random colour transformations (hue, saturation and brightness). The dataset is split into testing and training data.

Step 2.   Construction of ResNet101 Model and Feature Extraction

Regarding the extraction of high-level features from each image, the pre-trained on ImageNet ResNet101 was exploited with the use of Transfer learning to further alleviate data scarcity. The fully connected layers of the ResNet101 are replaced with new dense layers empirically designed for the custom task. The model is trained and fine-tuned in the corresponding shuffled training dataset. A validation split is also applied to monitor training. The features are then extracted from the last fully connected layer of the fine-tuned model and are separated according to their class. Lastly, the feature vectors are normalized in [0,1].

Step 3.   Construction of FCM

Based on the training set of images of the corresponding dataset, the input nodes of the graph are constructed. This is performed by clustering the deep feature representations extracted from the images utilizing the K-means algorithm, where the centroid of each cluster represents an input concept. The input nodes of the proposed Deepk-FCM represent semantic concepts, as they are illustrated in different images and are considered as Semantic Granules (SGs), where

clusters of images share similar characteristics. The generated centroids contain valuable information about each cluster. The output concepts of the proposed model are equal to the number of classes defined in the corresponding classification problem.

Among the input concepts, interconnections are determined to define the cause-and-effect relations between them. Traditionally, concepts and causal relations are defined based on the opinions of experts. However, in the proposed DeepK-FCM, the knowledge of experts is replaced by the similarities (2) between the extracted feature vectors and clusters' centroids, according to the following formula [19]:

$$d_{n,m}^{z,z\prime} = 1 - \frac{dist(f_{n,z}, g_{m,z\prime})}{\sum_{z=1}^{Z} \sum_{j=1}^{M_j} dist(f_{n,z}, g_{j,z\prime})} \qquad (2)$$

where *dist* represents the Euclidean distance, $f_{n,z}$ demonstrates the feature vectors, *n* displays the number of images, and *z, z' = 1, …, Z*, with *Z* the total number of output classes. With respect to $g_{m,z\prime}$, it defines the calculated centroids of the corresponding clusters, and *m* is the value of centroids for each class. The similarities can be considered as different opinions from experts, and in our case, they are defined by the training images.

Subsequently, the similarities are fuzzified with the use of triangular membership functions in [0,1] universe of discourse. To acquire the weight matrix, the fuzzy similarities values of all training feature vectors are gathered. In more detail, each training feature vector is considered an expert and its "opinion" is aggregated [18]. This opinion, as previously stated, represents the fuzzy similarity values between each centroid. For the weight between input concepts, the following formula (3) is applied [11]:

$$w_{ij} = \frac{\sum_{n=1}^{N_i} d_{n,i}^{m,i} \cdot \mu_{i,j}\left(d_{n,i}^{m,i}\right) + \sum_{n=1}^{N_j} d_{n,j}^{m,j} \cdot \mu_{i,j}\left(d_{n,j}^{m,j}\right)}{\sum_{n=1}^{N_i} \mu_{i,j}\left(d_{n,i}^{m,i}\right) + \sum_{n=1}^{N_j} \mu_{i,j}\left(d_{n,j}^{m,j}\right)} \qquad (3)$$

where $\mu_{i,j}\left(d_{n,i}^{m,i}\right)$ is the membership value of each fuzzy variable, based on the union operation (*U*) for overlapping fuzzy variables. Concerning the weights between an input and an output concept, symbolized as $\widehat{w}_{ij}$, these are computed according to (4):

$$\widehat{w}_{ij} = \frac{\sum_{n=1}^{N_i} d_{n,i}^{m,i} \mu_{m,i}\left(d_{n,i}^{m,i}\right)}{\sum_{n=1}^{N_i} \mu_{m,j}\left(d_{n,i}^{m,i}\right)} \qquad (4)$$

Step 4.   DeepK-FCM Inference

During inference, the testing data are prepared according to the first step and are passed to the ResNet101 to acquire a feature vector. The similarities between the new feature vector and the computed centroids of the training dataset are then calculated with Eq. (3) to acquire the initial concepts values. Following the proposed methodology with fuzzy clustering of similarities, the causal relationships among FCM concepts are defined and the produced FCM model of step 3 is utilized for decision making. Finally, FCM inference is performed with Eq. (1) till the convergence of the concept states. The output concept that has the highest activation state indicates the class the data belongs to. An example of the FCM inference process for the binary classification problem with 2 centroids for each class is presented in Fig. 3.
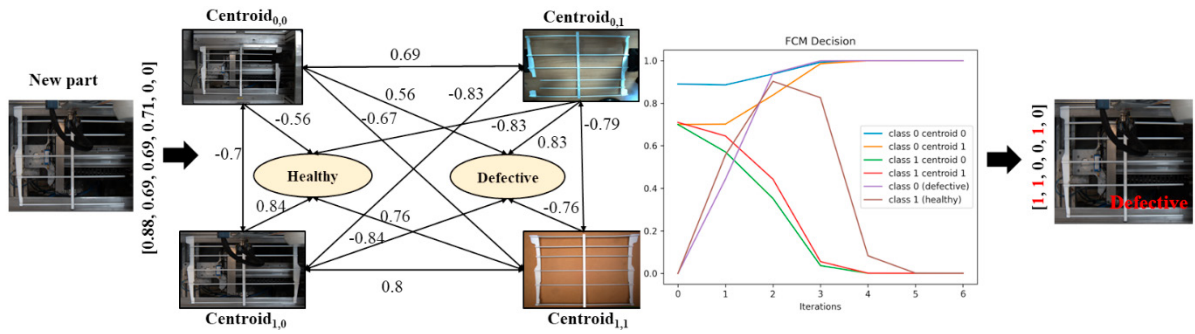
Fig. 3. The FCM decision for the binary classification problem with 2 centroids for each class. The similarities between the features of a new part and the centroids are calculated and passed as concepts to the FCM. The FCM converged in a state where class 0 (purple line) is high, whereas class 1 is low (brown line).

4. Results and discussion

The experiments were implemented in Python 3.10 using the TensorFlow 2.9.1 framework on a workstation with Intel Core i9-11900KF @ 3.5GHz CPU, 16 GB RAM and NVIDIA GeForce RTX 3080 Ti with 12GB of GDDR6X memory.

Initially, the potentials of CNNs models for this task were examined. For direct comparison, all CNN models received the same training and head parameters that were chosen empirically. In detail, a global max pooling layer and two fully connected layers with 1024 and 512 neurons were inserted on top of the CNNs. To avoid overfitting, dropout layers were utilized between the fully connected layers with 20% probability. The output layer consisted of one neuron with sigmoid activation function, hence the log loss function was employed for penalizing learning. In addition, to facilitate learning for the minority class, a higher weight of 1.2 for the defective parts was passed to the loss function. The training was performed in two stages. The Adam optimizer [20] with learning rate of 0.001 was implemented for the first stage, in which only the weights of the fully connected layers were trained so as not to distort the already learned parameters of the CNNs. Subsequently, in the second stage, the whole model was fine-tuned with a low learning rate of 10^{-6} in Adam. A validation split of 20% was performed in the training dataset to terminate learning with an early stopping algorithm, in case of overfitting. Finally, 10 instances of each model were trained for this task to ensure the validity and repeatability of the obtained results. The results of the four pre-trained CNN models that were examined in terms of the average binary accuracy, the average Area Under Curve (AUC) and the time per training step with 8 batch size are presented in Table 1.

Table 1. The results of CNN models in terms of average Accuracy for 10 runs, average AUC and time per step for the fine-tuning of the whole model.

CNN model	Binary Accuracy	AUC	Time per Step (ms)
VGG-16	0.760 ± 0.006	0.842 ± 0.077	308
VGG-19	0.763 ± 0.008	0.842 ± 0.080	356
ResNet50	0.763 ± 0.005	0.850 ± 0.041	210
ResNet101	0.769 ± 0.006	0.849 ± 0.049	340

It is observed that all CNN models produced similar metrics. Moreover, the maximum accuracy that was reached during experiments was 0.778, which indicates limitations concerning data, as all models struggled to identify the class for the same antenna parts.

In what follows, DeepK-FCM methodology was assessed. Assuming the full potentials of the CNN feature extractor were reached with the ResNet101 model that achieved the highest metrics, DeepK-FCM performance was then susceptible to the number of clusters and the l-slope sigmoid (2) parameter in FCM inference; therefore,

experiments were performed with different values for these parameters. Moreover, besides the number of clusters K that was being altered during experiments, all other parameters were the default ones from the implementation of the K-Means algorithm in the scikit-learn python library. Obviously, the same training and testing sub-datasets were employed for the assessment of DeepK-FCM as with the CNN implementation. A synopsis of the experiments is presented in the following Table 2.

Table 2. The results of CNN models in terms of Accuracy and AUC.

Number of clusters	Sigmoid slope	Binary Accuracy	Precision	Recall
2	1	0.500	0.500	1.000
	5	**0.805**	**0.736**	**0.944**
	10	0.764	0.694	0.944
4	1	0.778	0.717	0.917
	5	0.778	0.717	0.917
	10	0.778	0.717	0.917
6	1	0.778	0.717	0.917
	5	0.778	0.717	0.917
	10	0.778	0.717	0.917
8	1	0.778	0.717	0.917
	5	0.778	0.717	0.917
	10	0.778	0.717	0.917

It is exhibited that as the number of classes increased the DeepK-FCM reached the data limitation that was also presented in the CNNs assessment. However, when the number of clusters was set to 2, DeepK-FCM managed to increase the binary accuracy in the test dataset by almost 3%, yet it presented sensitivity in the sigmoid slope parameter. To further understand the behavior of DeepK-FCM, its explainable abilities could be exploited. Moreover, DeepK-FCM can provide a more explainable result than CNNs as, based on the criteria that were defined in this survey [21], it is both able to uncover the patterns within the inner mechanism of the classifier and to further explain the decisions made by the algorithm. In more detail, initially, the calculated similarities could be analyzed as these contributed to the initialization of the fuzzy sets and consequently to the weight matrix. The fuzzy sets of the similarities for 2 centroids are presented in Fig. 4., the peaks of the triangles correspond to the minimum, the average and the maximum similarity values that were found in the training dataset. These similarities practically explain how comparable antennas from different clusters are, based on the patterns that the CNN identifies in the dataset. Ideally, a similarity vector in the form of [d1, d2, d3, d4], where d1, d2, d3, d4 $\in$ [0,1], would have [d1, d2] $\subseteq$ "high" and [d3, d4] $\subseteq$ "low" for an image that belongs to *class 0* and vice versa.
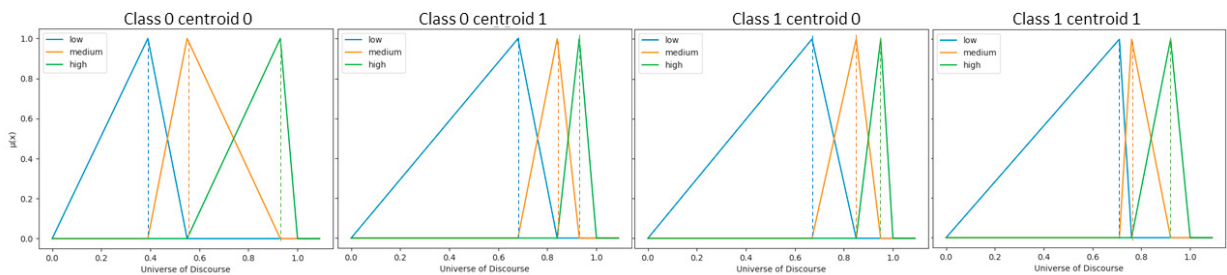

Fig. 4. The fuzzy sets of the similarities between feature vectors and centroids for 2 clusters and 2 classes.

To this end, the internal classification procedure came to light with the derived weight matrix of Table 3 and the similarities vector. Correspondingly, the derived weight matrix along with the equation (1) explains the decision made by the classifier as it was presented previously in Fig. 3. As a result, it was concluded that the misclassified parts were the product of similarities with the largest deviation vectors, and that the underlying CNN feature extractor completely failed to distinguish their structure. In addition, DeepK-FCM managed to increase the accuracy for the parts whose similarities vectors were analogous.

Table 3. The derived weight matrix.

	Class 0 centroid 0	Class 0 centroid 1	Class 1 centroid 0	Class 1 centroid 1	Class 0 (defective)	Class 1 (healthy)
Class 0 centroid 0	0	0.69	-0.70	-0.67	0.56	-0.56
Class 0 centroid 1	0.69	0	-0.83	-0.79	0.83	-0.83
Class 1 centroid 0	-0.70	-0.83	0	0.80	-0.84	0.84
Class 1 centroid 1	-0.67	-0.79	0.80	0	-0.76	0.76
Class 0 (defective)	0	0	0	0	0	0
Class 1 (healthy)	0	0	0	0	0	0

5. Summary

In this work, the quality inspection of the antenna assembly was examined as a binary classification task for imagery data using the innovative methodology of DeepK-FCM with explainability features (. A real industrial and scarce dataset was exploited to develop and test a transparent classifier that incorporates Transfer learning, Deep Convolutional Networks for feature extraction, a clustering algorithm, and Fuzzy Cognitive Maps as an explainable model for final decision making. The developed model, DeepK-FCM, managed to increase the accuracy of the fine-tuned Convolutional Networks by 3% and at the same time it succeeded to uncover the internal classification procedure. Moreover, DeepK-FCM presents an easy generic framework, as the nodes of the Fuzzy Cognitive Maps were the cluster centroids of the feature vectors, whereas the weight matrix (means the causal interconnections among nodes) was acquired based on the similarities of each image and the corresponding centroids. Furthermore, as a generic framework, the proposed method can be applied to other industrial domains that aspire to incorporate explainable models into their quality inspection procedure.

The limitations of this work are closely related to the data scarcity of the examined industrial dataset; therefore, the proposed methodology will be re-evaluated when more data will be available as well as other real industrial datasets will be involved. In fact, the generalization ability of this approach in a variety of real industrial datasets would provide an insight in the practical implications and the challenges that need to be addressed in other domains. Furthermore, future work will be focused on the investigation of evolutionary learning algorithms for FCM weight matrix optimization after fuzzy clustering. Concerning the concept definition, different methods will be further examined that would present even more transparency of the underlying system, as DeepK-FCM still relies on the obscure feature vectors of the Convolutional Networks.

References

[1]   L. Leontaris, A. Mitsiaki, P. Charalampous, N. Dimitriou, E. Leivaditou, A. Karamanidis, G. Margetis, K.C. Apostolakis, S. Pantoja, C. Stephanidis, others, A blockchain-enabled deep residual architecture for accountable, in-situ quality control in industry 4.0 with minimal latency, Computers in Industry. 149 (2023) 103919.

[2]   J. Wang, Y. Ma, L. Zhang, R.X. Gao, D. Wu, Deep learning for smart manufacturing: Methods and applications, Journal of

Manufacturing Systems. 48 (2018) 144–156.

[3]   J. Deng, W. Dong, R. Socher, L.-J. Li, K. Li, L. Fei-Fei, ImageNet: A large-scale hierarchical image database, in: 2009 IEEE Conference on Computer Vision and Pattern Recognition, 2009: pp. 248–255. https://doi.org/10.1109/CVPR.2009.5206848.

[4]   S. Kornblith, J. Shlens, Q.V. Le, Do better imagenet models transfer better?, in: Proceedings of the IEEE/CVF Conference on Computer Vision and Pattern Recognition, 2019: pp. 2661–2671.

[5]   K. Simonyan, A. Zisserman, Very deep convolutional networks for large-scale image recognition, arXiv Preprint arXiv:1409.1556. (2014).

[6]   K. He, X. Zhang, S. Ren, J. Sun, Deep Residual Learning for Image Recognition, (2015). https://doi.org/10.48550/ARXIV.1512.03385.

[7]   P. Angelov, E. Soares, Towards explainable deep neural networks (xDNN), Neural Networks. 130 (2020) 185–194.

[8]   B. Kosko, Fuzzy cognitive maps, International Journal of Man-Machine Studies. 24 (1986) 65–75.

[9]   E.I. Papageorgiou, Learning Algorithms for Fuzzy Cognitive Maps—A Review Study, IEEE Transactions on Systems, Man, and Cybernetics, Part C (Applications and Reviews). 42 (2012) 150–163. https://doi.org/10.1109/TSMCC.2011.2138694.

[10] E.I. Papageorgiou, Fuzzy cognitive maps for applied sciences and engineering: from fundamentals to extensions and learning algorithms, Springer Science & Business Media, 2013.

[11] G. Sovatzidi, M.D. Vasilakakis, D.K. Iakovidis, Automatic Fuzzy Graph Construction For Interpretable Image Classification, in: 2022 IEEE International Conference on Image Processing (ICIP), 2022: pp. 3743–3747. https://doi.org/10.1109/ICIP46576.2022.9897471.

[12] T. Tziolas, T. Theodosiou, K. Papageorgiou, A. Rapti, N. Dimitriou, D. Tzovaras, E. Papageorgiou, Wafer Map Defect Pattern Recognition using Imbalanced Datasets, in: 2022 13th International Conference on Information, Intelligence, Systems & Applications (IISA), 2022: pp. 1–8. https://doi.org/10.1109/IISA56318.2022.9904402.

[13] A.M. Hilal, H. Alsolai, F.N. Al-Wesabi, M.K. Nour, A. Motwakel, A. Kumar, I. Yaseen, A.S. Zamani, Fuzzy cognitive maps with bird swarm intelligence optimization-based remote sensing image classification, Computational Intelligence and Neuroscience. 2022 (2022).

[14] E.I. Papageorgiou, A new methodology for Decisions in Medical Informatics using fuzzy cognitive maps based on fuzzy rule-extraction techniques, Applied Soft Computing. 11 (2011) 500–513. https://doi.org/10.1016/j.asoc.2009.12.010.

[15] E.I. Papageorgiou, N.I. Papandrianos, D.J. Apostolopoulos, P.J. Vassilakos, Fuzzy cognitive map based decision support system for thyroid diagnosis management, in: 2008 IEEE International Conference on Fuzzy Systems (IEEE World Congress on Computational Intelligence), IEEE, 2008: pp. 1204–1211.

[16] E.I. Papageorgiou, A. Kannappan, Fuzzy cognitive map ensemble learning paradigm to solve classification problems: Application to autism identification, Applied Soft Computing. 12 (2012) 3798–3809. https://doi.org/10.1016/j.asoc.2012.03.064.

[17] E.I. Papageorgiou, K.E. Parsopoulos, C.S. Stylios, P.P. Groumpos, M.N. Vrahatis, Fuzzy Cognitive Maps Learning Using Particle Swarm Optimization, J Intell Inf Syst. 25 (2005) 95–121. https://doi.org/10.1007/s10844-005-0864-9.

[18] G. Sovatzidi, M.D. Vasilakakis, D.K. Iakovidis, IF3: An Interpretable Feature Fusion Framework for Lesion Risk Assessment Based on Auto-constructed Fuzzy Cognitive Maps, in: S. Ali, F. van der Sommen, B.W. Papież, M. van Eijnatten, Y. Jin, I. Kolenbrander (Eds.), Cancer Prevention Through Early Detection, Springer Nature Switzerland, Cham, 2022: pp. 77–86. https://doi.org/10.1007/978-3-031-17979-2_8.

[19] M.D. Vasilakakis, D.K. Iakovidis, Fuzzy similarity phrases for interpretable data classification, Information Sciences. 624 (2023) 881–907. https://doi.org/10.1016/j.ins.2023.01.009.

[20] D.P. Kingma, J. Ba, Adam: A method for stochastic optimization, arXiv Preprint arXiv:1412.6980. (2014).

[21] E. Tjoa, C. Guan, A Survey on Explainable Artificial Intelligence (XAI): Toward Medical XAI, IEEE Transactions on Neural Networks and Learning Systems. 32 (2021) 4793–4813. https://doi.org/10.1109/TNNLS.2020.3027314.